Preprints of the 19th World Congress
The International Federation of Automatic Control
Cape Town, South Africa. August 24-29, 2014

Analysis of the applicability of PMD cameras for measuring altitude of flight near undisturbed water surface

Dmitriy Krysin, Alexander Nebylov

State University of Aerospace Instrumentation, 67 Bolshaya Morskaya, 190000, Saint Petersburg, Russia. (Tel: +7(812) 494-70-16; e-mail: wtxt@ya.ru)

Abstract: Landing on undisturbed surface of water is one of the most specific and complex elements of piloting seaplanes. The main reason for this is the complexity of visual assessment of altitude. Analysis showed that most of the existing methods and systems for contactless measurement of distance cannot be used for measuring flight altitude with required accuracy near water surface. Radio altimeters have the most suitable characteristics, however, for economic reasons, they are not installed on all seaplanes. Lack of accurate instrument information about the most important navigation parameter negatively affects the safety of flights. Above facts point to the importance of finding new methods of measuring flight altitude near undisturbed surface of water. For solving this problem, the paper focuses on analyzing the applicability of time-of-flight cameras, which are based on the Photonic Mixer Device (PMD) technology. The paper presents preliminary experimental results that confirm the possibility of using a static PMD camera for altitude measurement near undisturbed surface of water. Further, during landing the vertical velocity component and angular velocity of an aircraft do not have high values. The horizontal velocity component does not affect the view of range images in case of undisturbed water surface. Therefore an inference is made that PMD cameras can be used for measuring altitude of flight near undisturbed water surface.

Keywords: Altitude measurement, water surface, time-of-flight, PMD camera, range image

1. INTRODUCTION

The control of seaplanes has several features in comparison with the control of land airplanes and requires special training and skills (Nebylov, 2011). One of the most specific and complex elements of piloting a seaplane is landing on the undisturbed surface of water. The main reason is the difficulty of visual estimation of flight altitude. When landing in such conditions, the pilot must be guided by the instrument readings, as well as overwater and landmarks. The measurement error of the altitude should not exceed 0.5 m for a normal landing. Meanwhile, the majority of existing instruments for contactless distance measurement do not provide such accuracy and cannot be used for measurement of flight altitude near water surface.

Barometric altimeters have unacceptable instrumental error for the landing, which can reach 10 meters at zero altitude.

GPS-receivers also do not provide the required accuracy of altitude measurement. The standard deviation in the non-differential mode is about 3 m. Furthermore, the altitude is determined with respect to a model of the Earth, while the level of water surface is generally subjected to variations.

Laser rangefinders are usually based on the use of collimated light. In the general case, only a small portion of the incident laser radiation is reflected in the direction of the receiver from water surface. This may lead to unacceptably weak signal at the receiver input and instability of the measurement process.

Ultrasonic rangefinders have a number of drawbacks. The main disadvantage is the dependence of the sound velocity on the air parameters that affects the accuracy. Furthermore, the possibility of measurement strongly depends on the spatial position of the ultrasonic rangefinder relative to the probed surface.

Radio altimeters provide the required measurement accuracy. They are widely used in large seaplanes as main instrument for flight altitude measurement during the landing. However, the use of radio altimeters in small seaplanes is often impractical from the economic point of view. Lack of accurate instrument information about the most important navigation parameter negatively affects the safety of flights.

Above facts point to the importance of finding new methods that provide an autonomous measurement of flight altitude near undisturbed surface of water.

Recently there has been a rapid expansion of application of machine vision methods and systems. This tendency is primarily associated with increase of performance of computing means and creation of new types of sensors. Time-of-flight cameras are one of such new sensors (Piatti and Rinaudo, 2012, Ringbeck and Hagebeuker, 2007). They allow getting range images containing information about the distance to the objects in the camera field of view.

At the moment, there is a number of publications that address the issue of using time-of-flight cameras in the case when the scene contains transparent objects, including water (Hansard et al., 2012, Kohoutek et al., 2012, Moranski, 2011, Nitsche et al., 2010). Nevertheless, the problem of measurement of

distance to water surface is not considered therein. This article partly fills the gap. It is devoted to an analysis of the applicability of time-of-flight cameras for flight altitude measurement near undisturbed surface of water.

2. PHOTONIC MIXER DEVICE

Currently, it is very hard to find range images in the public domain. This can be explained by the novelty of the technology and specific formats of the range images. As a result, at an initial phase of the study real range images of the undisturbed water surface were obtained to confirm the possibility of application of time-of-flight cameras. A time-of-flight camera, based on the Photonic Mixer Device (PMD) technology, was used.

2.1. Description of PMD technology

PMD technology is based on time-of-flight method of distance measurement. The method consists of measuring the time that is necessary for light signal to travel the distance between the camera and a reflective object. PMD cameras illuminate the scene using modulated infrared light with a modulation frequency f_{mod}. Infrared light reflects from objects and is measured by PMD camera image sensor (photosensitive matrix). Further, special circuitry calculates the phase shift φ between the emitted and the received signal, which is proportional to the distance D to the object:

$$D = \frac{c\varphi}{4\pi f_{mod}}, \quad (1)$$

where c - speed of light. Every element of the photosensitive matrix has its own signal. Therefore, the distance for each pixel is computed independently. As a result PMD camera produces an image that is a 3D-model of the scene in the camera field of view. In the literature there are different names of such images: range images, depth maps, 3D images. In this paper the term "range image" is used.

In this way unlike stereo vision systems, PMD cameras allow obtaining range information without resorting to the methods of acquisition and analysis of stereoscopic images. Furthermore unlike the laser scanners, PMD cameras do not use moving mechanical elements. Complex and computationally intensive algorithms are not required. The latest models of PMD cameras are able to transmit to the control device completely ready range images at the rates up to 90 Hz.

At the same time, PMD cameras have limitations. The maximum measured distance is the ratio of the speed of light to twice the modulation frequency. The resolution of range images is relatively small. The measurement accuracy depends on a number of factors. More information on features of PMD cameras can be found in (Piatti and Rinaudo, 2012, Ringbeck and Hagebeuker, 2007).

2.2. Formats of range images

PMD camera provide several formats of range images.

Initially the distance is measured in a spherical coordinate system with the origin at the focus of the camera optical system. Only one matrix (array of numbers) is needed to store corresponding original range image. The elements of this matrix contain estimates of the radial distance to the surface of the scene (in meters). The number of matrix elements is equal to the number of sensitive elements of the PMD sensor.

PMD camera intrinsic parameters (focal length and coordinates of principal point) are determined during the production. Thus from radial distances PMD camera can automatically calculate the coordinates of the corresponding points in three-dimensional Cartesian coordinate system. Three matrices are needed for storing the corresponding image (one for each coordinate). The matrices have the same size as the original range image. Obviously, range images in format of points in Cartesian coordinate system are more informative.

Range images generated by the PMD camera may contain valid and invalid pixels. Valid pixels are the pixels that contain distance measurements in meters. Invalid pixels contain codes of errors instead of distance measurements, which lead to inability of measurement. There are two main errors: saturation (code -1) and weak signal (code -2).

3. EXPERIMENTS AND RESULTS

Obviously, practical implementation of an experiment for testing the measurement system on a dynamic object is much more difficult than an experiment on a static object. At the same time experiment on a dynamic object, probably makes no sense, if the measurement system could not work even on a static object. Therefore it was decided to split the experiments on the applicability of PMD cameras for flight altitude measurement near water surface into two stages. The first stage is testing of PMD cameras on a static object, and the second stage is testing of PMD cameras on a dynamic object. At the moment the first stage has been completed. Results are discussed below.

3.1 Experimental setup

The developed experimental setup includes the following major components: PMD camera O3D201 manufactured by IFM (Fig. 1), personal computer, power supply, and a tripod. A general view of the setup is presented in the next section in Fig. 2. Main features of PMD camera O3D201 are presented in table 1.

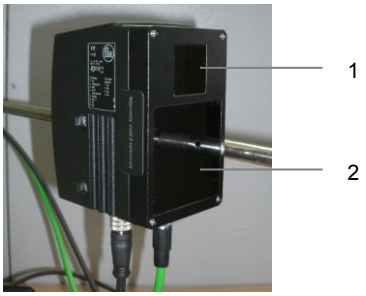

Fig. 1. PMD camera O3D201: 1 – window of the image sensor, 2 – window of the source of infrared light)

Table 1. Features of the PMD camera O3D201

Sensor type	PMD 3D chip
Range limit	6.5 m
Illumination unit	Infrared LEDs (850 nm)
Image resolution	50 x 64 pixels
Viewing angles	30° x 40°
Maximum frame rate	20 Hz
Data Interface	Ethernet 100Base-TX
Power supply	24 V ± 10 %

The systematic component of PMD camera measurement error depends strongly on the accuracy of calibration. The random component can be much higher than systematic and depends on a number of external factors (Nitsche, 2010). The following factors lead to its increase: small amplitude of the reflected signal, high intensity of the ambient light, motion of objects in the scene, small exposure time of PMD camera, usage of another PMD camera with the same modulation frequency nearby. The amplitude of reflected signal depends on the distance to objects and their reflectivity. The presence of surfaces with high reflectivity can lead to saturation of the sensor elements and impossibility of measurement. As an example, Table 2 shows the typical confidence intervals of the PMD camera O3D201, taken from its datasheet.

Table 2. Typical confidence intervals of the PMD camera O3D201

Range [m]	Typical confidence intervals (±3σ) [mm]		
	Reflectivity 0.9 (white surface)	Reflectivity 0.18 (grey surface)	Reflectivity 0.06 (black surface)
0.5	±5	±8	±16
2	±6	±9	±20
5	±8	±24	±74

The table shows that the value of the confidence interval increases with increasing range and reducing surface reflectivity. The documentation on the PMD camera O3D201 does not include the confidence intervals for the surfaces with reflectivity less than 0.06. It should be noted that for vertical incidence of optical radiation from the air to water surface the reflection coefficient equals to 0.02. Therefore, the possibility of using of PMD cameras for measurement of range to water surface was in question before the experiments.

The described experimental setup was used to obtain real range images of the mirror-like surface of water. Experiments were carried out both in the laboratory and outdoors. The results that were obtained outdoors are particularly valuable, since in real natural conditions a complete absence of waves on water surface is extremely rare and does not continue for a long time. More often one can see water surface in a state that is close to the completely undisturbed state, but, little waves and ripples still appear periodically. The experiment that is described in the following subsections was made in such conditions.

3.2. Description of an experiment at the river

The setup was installed on the bridge (Fig. 2). The depth of the river at the place of the experiment is 1–1.5 m. Weather: partly cloudy, almost no wind. Wave heights did not exceed 0.05 m, that corresponds to 1 point on the scale of Douglas (Faltinsen, 1990). Optical properties of the water surface were similar to the properties of a flat mirror (from the viewpoint of directions of reflected optical rays). This is confirmed by the reflection of buildings that are visible in Fig. 2. Acquisition of range images was performed at two different PMD camera positions with different altitudes. The altitude of the first camera position relative to the water surface was measured using a tape measure and a plumb and was 5.7 m. The altitude of the second position is 5.82 m. Camera was rotated at an angle 5–10° around an axis that is parallel to the short side of the image sensor. This was done to avoid entering bridge construction in the PMD camera field of view.

Fig. 2. Experimental setup and conditions of the experiment (St. Petersburg, Fontanka river, English footbridge)

During the experiment sequences of range images of the water surface were obtained at each of the PMD camera positions. Each sequence was obtained at a fixed exposure time and contains 100 range images. Exposure time was set in the range from 0.1 to 5.0 ms. The frequency of range image acquisition was about 2 Hz. The images were obtained in the format of radial distances, and in the format of points in Cartesian coordinate system.

3.3. Range images of undisturbed surface of water

As an example, Fig. 3 (a) shows a range image of the water surface in the format of radial distances. Image was obtained at the altitude of 5.7 m. Exposure time of 2 ms was used. The values of valid and invalid pixels are coded in color. White and black areas contain invalid pixels. White area is the invalid pixels with code -2 (weak signal). Black area is the invalid pixels with code -1 (saturation). A key feature of the displayed range image is a small region of valid pixels with distance measurements to the water surface. This region is only a few percent of the total range image area. A fragment of this range image with the region of valid pixels is shown in Fig. 3 (b). One can see that the valid pixels contain range measurements, that are close to the actual value of the

altitude 5.7 m. The region is shifted to the lower side of the image because of the described tilt of the PMD camera.

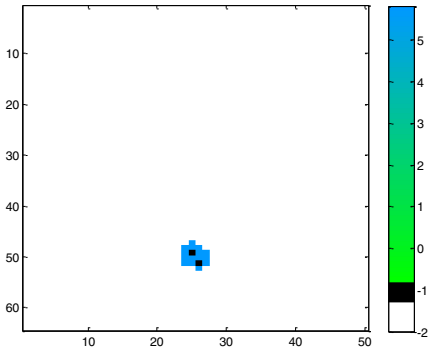

(a) Range image of the water surface

-2	-2	-2	-2	-2	-2
-2	-2	5,782	-2	-2	-2
-2	5,711	5,758	5,813	-2	-2
-2	5,709	-1	5,732	5,760	-2
-2	5,743	5,746	5,735	5,820	-2
-2	5,712	5,711	-1	5,769	-2
-2	-2	-2	5,786	-2	-2
-2	-2	-2	-2	-2	-2

(b) Fragment of the range image

Fig. 3. (a) Two-dimensional visualization of range image in format of radial distances; (b) Fragment of this image with the region of valid pixels. Image was not processed

Fig. 4 shows a cloud of points constructed of valid pixels of the same range image, but in format of points in Cartesian coordinate system. This figure allows us to estimate an actual size of the water surface area, that corresponds to the region of valid pixels in the range image (Fig. 3).

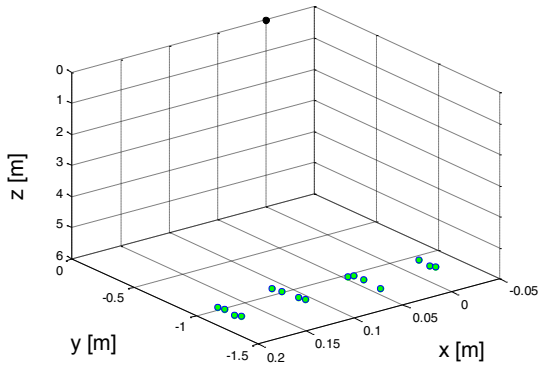

Fig. 4. Cloud of points constructed of valid pixels of the same range image, but in format of points in Cartesian coordinate system

3.4. Formation of range images of water surface

The distance between the IR emitter and the PMD camera image sensor is not large in comparison with the measured distance. Reflection of rays from the mirror-like surface of water is described by the specular reflection of light (Martin, 2004). The infrared light is reflected towards the sensor only from a limited area of the mirror-like surface of water. The rays fall on this area at small angles. Fig. 5 illustrates this statement. The large number of invalid pixels can be explained by the fact that a significant part of infrared radiation from the corresponding surface areas is not reflected in the direction of the PMD camera. Tilting of the PMD camera leads to the displacement of the region of valid pixels in the corresponding range images.

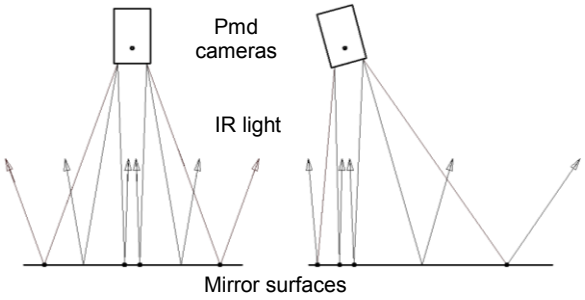

Fig. 5. Operation of PMD cameras over mirror surfaces

In case of increasing the intensity of water surface disturbance, the number of areas on which the rays of IR light fall at small angles also increases. This statement was confirmed experimentally (Fig. 6).

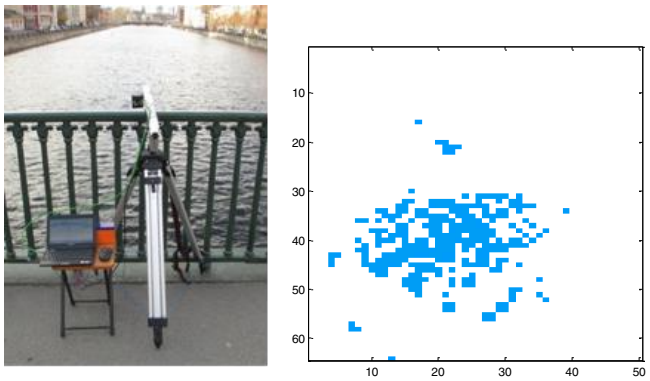

(a) (b)

Fig. 6. (a) Another experiment at the same place but over more intense disturbance of the water surface. (b) View of the corresponding range image (one can see the difference from the image presented in Fig. 3)

3.5. Processing of range image sequences

Fig. 7–8 show the results of statistical processing of a sequence of 100 water surface range images. This sequence was obtained at altitude of 5.7 m. Exposure time of 2 ms was used. Range image shown in Fig. 3–4 was taken from this sequence.

Histogram of valid pixels distribution of sequence images has a distinct maximum near the actual value of the altitude of 5.7 m (Fig. 7). A slight shift of the peak can be explained by the fact that most of the valid pixels of range images contain measurements of slant range, not the altitude.

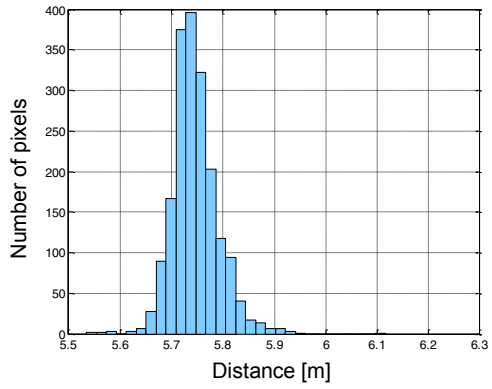

Fig. 7. Histogram of the distribution of valid pixels

Fig. 8 shows maximum, mean, median, and minimum values of valid pixels of each range image of the same sequence. Actual altitude is also shown. Analysis of the plot leads to the conclusion that, the region of valid pixels is stably present in all obtained range images of the water surface despite its small area. As a simple, but a rough estimate of the altitude, it is possible to use the average or median value of all valid pixels of the range image. Suppose that the mean value of all valid pixels of the range image is used as an estimate of the altitude. The mean value of such estimate for presented sequence is 5.744 m. Its standard deviation is 0.017 m (less than two centimeters). A better estimate with a smaller standard deviation can be obtained by using subsequent filtering. For example, the basic Kalman filter can be used (Welch and Bishop, 1995, Bradski and Kaehler, 2008). Obviously, in the general case such estimate is higher than actual value of the altitude, because during its calculation the measurements of slant ranges are summarized. A more accurate estimate can be obtained by introducing a correction weighting coefficient. Methods of its calculation under various operating conditions are in the process of developing.

Processing of range images obtained at the altitude of 5.82 m, showed that mean values of the estimates differ by about 0.12 m from the results obtained at the altitude of 5.7 m.

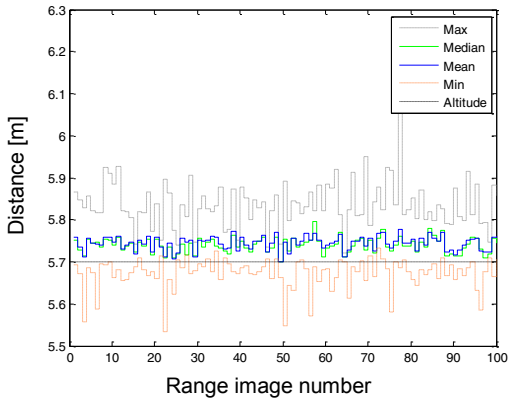

Fig. 8. Maximum, mean, median, and minimum values of valid pixels of each range image of the sequence. The sequence was obtained at exposure time of 2 ms

An experimental dependence of the number of valid and invalid pixels on the exposure time is presented in Fig. 9 (a).

Figure shows that the number of valid pixels increases with increasing exposure time. It is necessary to note that number of invalid pixels with code -1 also increases. The dependence of the ratio of the number of invalid pixels (with code -1) to the number of valid pixels on the exposure time for the same range image sequence is presented in Fig. 9 (b).

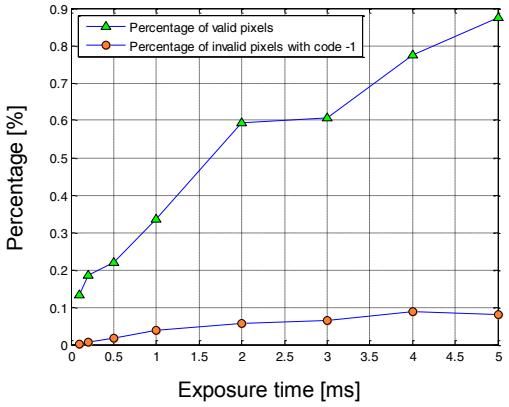

(a) Number of valid and invalid pixels

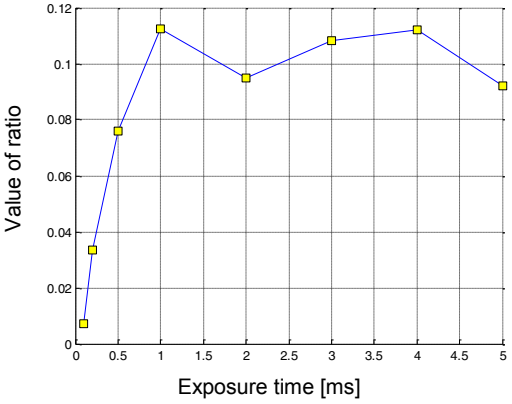

(b) Ratio of the number of invalid pixels (with code -1)
1) to the number of valid pixels

Fig. 9. (a) Experimental dependence of the number of valid and invalid pixel images on the used exposure time. Each point on the graph is the mean value of the relative number of pixels for the corresponding range image sequence; (b) Experimental dependence of the ratio of the number of invalid pixels (with code -1) to the number of valid pixels on the exposure time for the same range image sequence

3.6 Experiments in the laboratory

The results obtained in the laboratory, are similar to those described above. However it is necessary to describe one important fact. The infrared radiation can be reflected from the bottom of the reservoir and measured by the PMD camera. This can occur if the depth of the reservoir is relatively low and the bottom has high reflectivity. This can occur despite the fact that water absorbs infrared radiation well. As a result the measurement error of range to the water surface increases.

3.7 Estimation of angular orientation of the PMD camera

It was shown in subsections 3.3–3.4 that tilt of the PMD camera is the reason of displacement of the region of valid pixels in the corresponding range image. This fact leads to the conclusion that range images of the mirror-like surface of water may be used to estimate not only the altitude of an object but also its angular orientation.

4. APPLICABILITY ON DYNAMIC OBJECTS

During landing the vertical velocity component of an aircraft in principle should not have high value. The same can be said about angular velocities. Vertical velocity component is much smaller than the horizontal velocity component. Therefore, the landing process in a limited time frame can be seen as a horizontal flight. The horizontal velocity component must not affect the view of range images if the flight takes place above undisturbed water. This can be explained as follows. It was mentioned above that reflection of rays from the undisturbed water surface is described by the specular reflection of light. It is known that in case of specular reflection the change in the relative position of a point and its optical image occurs only when the distance to the mirror surface changes. Moving of an object in a plane parallel to the mirror surface does not change the distance between points of the object and the mirror. Similarly the horizontal movement of the PMD camera does not change the distance between PMD camera and mirror-like surface of water. Therefore, the horizontal movement of the PMD camera should not lead to a change of range images of undisturbed water surface.

Thus an assumption can be made that up to a limit the horizontal velocity component of an object will not have a significant effect on the formation of range images of the undisturbed water surface and results obtained in the dynamics during the flight will be close to the results of the static experiment. The key condition is the water surface should not be disturbed at the time of the range image acquisition.

It should be noted that the maximum measurable distance of PMD cameras depends on the modulation frequency of infrared light. In the above described experiments, the maximum measurable distance of the PMD camera is 6.5 meters.

5. CONCLUSIONS

The obtained experimental results confirm the applicability of PMD cameras for altitude measurement of aircraft near undisturbed water surface. The specific view of range images of water surface can be explained by optical properties of water.

The theoretical analysis led to an inference that up to a limit the horizontal velocity component of an object will not have a significant effect on the formation of range images of undisturbed water surface and results which will be obtained in the dynamic conditions during flight will be close to the results of the static experiment.

Further research on this topic will focus on studying the functioning of PMD cameras in a wider range of environmental conditions, development of adaptive software, testing PMD cameras in dynamic conditions (on a water transport).

ACKNOWLEDGEMENT

The work was supported by the Russian Foundation for Basic Research under the project 12-08-00076-a.

REFERENCES

Bradski, G. and Kaehler, A. (2008). *Learning OpenCV. Computer vision with the OpenCV library*. Oreilly, Sebastopol.

Hansard, M., Lee, S., Choi, O., and Horaud, R. (2012). *Time-of-Flight Cameras. Principles, Methods and applications*. Springer

Faltinsen, O. (1990). *Sea Loads on Ships and Offshore Structures*. Cambridge University Press.

Kohoutek, T., Nitsche, M., and Eisenbeiss, H. (2012). Geo-referenced mapping using an airborne 3D time-of-flight camera. *ISPRS Workshop Laser Scanning Archives*, volume XXXVIII-5/W12.

Martin, S. (2004) *An introduction to ocean remote sensing*. Cambridge University Press.

Moranski, M. (2011). Computer vision based navigation systems – requirements and proposed system idea. In *Challenges of modern technology*, 2 (2).

Nebylov, A. and Nebylov, V. (2011). *Seaplane Landing Smart Control at Wave Disturbances.* 18th IFAC World Congress, Proceedings, Milano.

Nitsche, M., Turowski, J., Badoux, A., Pauli, M., Schneider, J., Rickenmann, D., and Kohoutek, K. (2010). Measuring streambed morphology using range imaging. In Dittrich, Koll, Aberle, Geisenhainer (eds), *River Flow*, 1715-1722.

Piatti, D. and Rinaudo, F. (2012). SR-4000 and CamCube3.0 Time of light (ToF) Cameras: Tests and Comparison. *Remote Sensing*, 4, 1069-1089.

Ringbeck, T. and Hagebeuker, B. (2007). A 3d time of flight camera for object detection. In *Optical 3-D Measurement Techniques*.

Welch, G. and Bishop, G. (1995). *An Introduction to the Kalman Filter*. University of North Carolina, Department of Computer Science, TR 95-041